Transient Ocean Currents Induced by Wind and Growing Waves

JAN ERIK WEBER AND ARNE MELSOM

Institute of Geophysics, University of Oslo, Blindern, Oslo, Norway

(Manuscript received 16 October 1991, in final form 27 February 1992)

ABSTRACT

A theoretical nonlinear model for wind- and wave-induced currents in a viscous, rotating ocean is developed. The analysis is based on a Lagrangian description of motion. The nonlinear drift problem is formulated such that the solution depends on a linearly increasing eddy viscosity in the water, the wave-growth rate, and the periodic normal (or tangential) wind stress at the sea surface. Particular calculations are performed for surface-stress distributions and growth rates obtained from asymptotic analysis of turbulent atmospheric flow, where the Reynolds stress is modeled by an eddy-viscosity assumption. For growing waves the wave-induced current develops in time. The calculations are terminated when the steepness of the fastest-growing waves reach that of a saturated sea. At this point, the magnitude of the wave-induced surface current is 8–9 times larger than the friction velocity in the water, and the direction of the current is deflected 2°–10° to the right of the wave-propagation direction.

1. Introduction

The theory of mean currents induced by interfacial waves has attained surprisingly little interest in the literature. For the particular case of water waves propagating along the sea surface, Dore (1978a,b) appears to be the first to point out the importance of the viscosity of the air for the mean-drift calculations. In doing so, he modified the well-known result of Longuet-Higgins (1953), obtained by essentially assuming that a vacuum exists (zero shear stress) above the water. Using a Lagrangian description of motion and taking the earth's rotation into account, this problem was elaborated further by Weber and Førland (1990).

In the cited papers, the upper fluid (the air) had no mean motion apart from that associated with the waves themselves. The most interesting (and intriguing) problem from a geophysical point of view, however, is when a wind is blowing over the sea. This is because the wind is the source of energy for most high-frequency ocean surface waves. The linear problem of wave generation by the wind has received extensive attention during the past three decades, or so. It has been demonstrated that energy and momentum may be transferred to water waves through resonance with wind-advected pressure perturbations (Phillips 1957) or by shear instability depending on the curvature of the wind profile (Miles 1957). More recently, explicit models for air turbulence have shown that turbulent Reynolds stresses are also effective in generating water waves (Jackson and Hunt 1975; Knight 1977; Jacobs 1987).

Little has been done to investigate the mean drift current associated with wind-influenced waves, although attempts have been made. In that respect we mention the works by Weber (1983) and Jenkins (1986). In the former work one particular form of the variable surface stress was considered. This form was chosen in such a way as to prevent the wave amplitude from decaying (or growing) in time. The aim of the present paper is to generalize this theory. We allow for arbitrary variable surface wind stresses and growth/decay rates in the nonlinear solution for the drift velocity. These stresses and growth/decay rates cannot, of course, be determined explicitly unless a model for the physical processes in the air above the water is considered. As an example we use the results from the asymptotic analyses of Knight (1977) and Jacobs (1987) for turbulent flow, where the turbulent Reynolds stress is modeled by an eddy-viscosity assumption. This yields a fairly robust model for wave growth, which is not so sensitive to the coupling between phase speed and wind friction velocity as Miles' shear mechanism appears to be; see the discussion by Phillips (1977, p. 129).

2. Mathematical formulation

The formulation of the problem follows closely that of Weber (1983) and Weber and Førland (1990). We consider monochromatic waves propagating along an uncontaminated sea surface. The water and the air are taken to be semi-infinite, homogeneous, incompressible fluids. The whole system rotates about the vertical

Corresponding author address: Prof. Jan Erik Weber, University of Oslo, Institute of Geophysics, P.O. Box 1022, Blindern N-0315 Oslo, Norway.

axis with constant angular velocity $\frac{1}{2}f$, where f is the Coriolis parameter.

The mathematical description of the fluid motion will be Lagrangian, and the dependent variables of the problem are expressed as functions of the Lagrangian coordinates a, b, and c and time t. A Cartesian right-handed coordinate system is defined such that the x, y axes are situated at the undisturbed sea surface. The z axis is directed vertically upward, and the position of the surface is governed by $c = 0$ for all times. The displacements x, y, and z and pressure p are written as series expansions after an ordering parameter ϵ, which essentially is proportional to the wave slope (Pierson 1962).

We look at wind-generated gravity waves propagating along the x axis with frequency ω and wavenumber k. For the waves considered here, $\omega \gg f$. Hence, the effect of rotation can be neglected in the calculation of the primary wave field (Weber 1990).

Turbulence is taken to exist in the air as well as in the water. The turbulent Reynolds stress is modeled by an eddy-viscosity assumption. Specific results for the airflow can be obtained directly from the asymptotic analyses by Knight (1977) and Jacobs (1987). These will be used in section 5.

In the water (like in the air) the generation of turbulence is mainly associated with the action of the *mean* flow, where the mean is taken over one wave cycle for a single wave or as an ensemble average for a continuous spectrum. The waves themselves are only weakly affected by turbulence, manifested through a somewhat larger dissipation of wave energy. This may adequately be accounted for by introducing a small constant eddy viscosity ν_0, which, however, is larger than the molecular value.

The larger part of the turbulent eddy viscosity, that is, that part connected with the mean motion, is taken to vary linearly with depth (Madsen 1977), analogous to the classic result for turbulent flow over a flat plate. The eddy viscosity ν may then be written

$$\nu = \nu_0 - \kappa u_* c. \tag{2.1}$$

Here κ is Von Kármán's constant (≈ 0.4) and u_* is the friction velocity in the water. The form (2.1) for the near-surface eddy-viscosity variation seems to be consistent with various observational results (Shemdin 1972; Wu 1975; McLeish and Putland 1975; Thorpe 1986; Cheung and Street 1988).

In the present analysis we disregard the (possible) existence of an extremely thin (of order millimeter) laminar sublayer at the surface. By taking $u_* = 0$, however, and letting ν_0 represent the molecular value of the viscosity coefficient, results for a *laminar,* viscous ocean follow immediately from our analysis.

According to our adopted approach, the divergence of the turbulent Reynolds stress tensor in the ocean, $P^{(ij)}_{\text{turb}}$, may be written in Eulerian form:

$$\frac{1}{\rho}\frac{\partial}{\partial x_j} P^{(ij)}_{\text{turb}} = \nu_0 \nabla^2 \tilde{u}_i + \nu \nabla^2 \bar{u}_i + \frac{\partial \nu}{\partial x_j}\left[\frac{\partial \bar{u}_j}{\partial x_i} + \frac{\partial \bar{u}_i}{\partial x_j}\right] - \frac{2}{3}\frac{\partial}{\partial x_i} K_{\text{turb}}, \tag{2.2}$$

where u_i are the velocity components and the subscripts i, j range from 1 to 3, with the usual summation convention for repeated subscripts. Here variables with a tilde represent high-frequency wave motion, while the overbarred quantities are the mean flow. In (2.2) K_{turb} is the kinetic energy per unit mass of the turbulent fluctuations. In the forthcoming analysis this term will, according to common practice, be incorporated into the isotropic pressure without further comments. In our Lagrangian formulation $\tilde{u}_i$ will essentially be replaced by $\epsilon x^{(1)}_{it}$, and $\bar{u}_i$ by $\epsilon^2 \bar{x}^{(2)}_{it}$, where the subscript t denotes partial differentiation with respect to time.

By utilizing (2.2) for the turbulent Reynolds stress and converting to Lagrangian coordinates a, b, c the equations of motion become similar to those given by Jenkins (1987) except that now the variation of the eddy viscosity is related directly to the mean flow. For a further discussion of the eddy-viscosity assumption, reference is made to section 6.

Following Lamb (1932) or Weber and Førland (1990), the solutions in the water to $O(\epsilon)$, representing the primary wave field, are readily obtained as

$$x^{(1)} = -\frac{ik}{n}\left[e^{kc} - \frac{im}{k} B e^{mc}\right] e^{ika+nt}, \tag{2.3}$$

$$z^{(1)} = -\frac{k}{n}[e^{kc} - iBe^{mc}] e^{ika+nt}, \tag{2.4}$$

$$p^{(1)} = \frac{\rho}{n}[(n^2 + gk)e^{kc} - igkBe^{mc}] e^{ika+nt}. \tag{2.5}$$

Here g is the acceleration due to gravity, and

$$m^2 = k^2 + n/\nu_0. \tag{2.6}$$

The wavenumber k is here taken to be real. For the time dependence we assume

$$n = -i\omega + \beta, \tag{2.7}$$

where the frequency ω and the growth rate β are both real. If ν_0 is small, we obtain approximately

$$m = (1 - i)\gamma, \tag{2.8}$$

where $\gamma = (\omega/2\nu_0)^{1/2}$. For a given value of the wavenumber, the complex quantities n and B ($= B_r + iB_i$) are determined from the boundary conditions at the sea surface.

We denote the periodic parts of the normal and tangential wind stresses at the sea surface by σ and τ, respectively. Utilizing the same series expansions in ϵ for

these quantities as for the other dependent variables of the problem, we find

$$\sigma^{(1)} = -p^{(1)} + 2\rho\nu_0 z_{lc}^{(1)}, \quad c = 0 \tag{2.9}$$

$$\tau^{(1)} = \rho\nu_0(x_{lc}^{(1)} + z_{la}^{(1)}), \quad c = 0. \tag{2.10}$$

Here we have neglected the effect of capillarity. Introducing

$$\left(\frac{\sigma^{(1)}}{\rho}, \frac{\tau^{(1)}}{\rho}\right) = (\sigma_1, \tau_1)e^{ika+nt}, \tag{2.11}$$

we obtain from (2.10)

$$B = -\frac{i\tau_1}{\omega_0} + \frac{k^2}{\gamma^2}, \tag{2.12}$$

where $\omega_0^2 = gk$. Elimination of B between (2.9) and (2.10) finally yields

$$\sigma_1 - i\tau_1 = i\left(\frac{\omega^2 - \omega_0^2}{\omega_0}\right) - 2\left(\beta + \omega_0\frac{k^2}{\gamma^2}\right). \tag{2.13}$$

Equation (2.13) is a general relation (within linear theory) between the periodic normal and tangential wind stresses acting along the sea surface. The relation is general in the sense that it does not depend on how the motion in the air is modeled. The result (2.13) may also be obtained from Miles' calculations [1962, Eq. (2.16) for the deep-water limit].

The results presented here have been derived under the assumption that

$$\left.\begin{aligned} |\beta|/\omega &\ll 1 \\ k/\gamma &\ll 1 \end{aligned}\right\}. \tag{2.14}$$

They are both, for most oceanographic problems, very well fulfilled.

We denote the initial wave amplitude by ζ_0. Insertion to lowest order in the vertical displacement at the surface then yields for the ordering parameter

$$\epsilon = \zeta_0\omega/k, \tag{2.15}$$

as in Weber (1983). If the governing equations were nondimensionalized, scaling the perturbation displacements and velocities by ζ_0 and $\zeta_0\omega$, respectively, the equivalent nondimensional expansion parameter would be the wave steepness $\zeta_0 k$. This is assumed to be a small quantity in our analysis, and we shall not pursue the calculations beyond $O(\zeta_0^2 k^2)$.

From (2.13) we note that the wave growth rate is determined by the real part of σ_1 and the imaginary part of τ_1. Denoting the surface elevation by ζ, we obtain to lowest order from (2.4)

$$\zeta = \zeta_0 e^{\beta t}\sin(ka - \omega t). \tag{2.16}$$

Using (2.16), the normal and tangential wind stresses to $O(\epsilon)$ at the sea surface may be written from (2.11):

$$\left.\begin{aligned} \sigma_r &= \frac{\rho\omega}{k^2}[\sigma_{1_r}\zeta_a - \sigma_{1_i}k\zeta] \\ \tau_r &= \frac{\rho\omega}{k^2}[\tau_{1_r}\zeta_a - \tau_{1_i}k\zeta] \end{aligned}\right\}, \tag{2.17}$$

where subscripts r and i denote real and imaginary parts. We recognize then, from (2.13) and (2.17), that wave growth is associated with that part of the *normal* wind stress that is in phase with the surface *slope* ζ_a. A similar role is played by that part of the *tangential* wind stress that is in phase with the surface *elevation* ζ. These are, of course, well-known results. The important question, however, relates to which of these stress contributions dominates the generation process. Here it appears to be a widespread consensus in favor of the normal stress contribution (Phillips 1977; Chalikov and Makin 1990). This means that usually

$$|\tau_{1_i}| \ll |\sigma_{1_r}|. \tag{2.18}$$

We shall return to this question later when motion in the air is considered.

3. Equations for the mean current in the ocean

The problem to $O(\epsilon^2)$ is analogous to that described in Weber (1983). With the adopted form (2.2) for the Reynolds stress, we find for the mean horizontal flow in the water

$$\begin{aligned}(\nu_0 - \kappa u_* c)\bar{x}_{lcc}^{(2)} - \kappa u_*\bar{x}_{lc}^{(2)} - \bar{x}_{lt}^{(2)} + f\bar{y}_l^{(2)} \\ = -\frac{1}{\rho}\overline{p_a^{(1)}x_a^{(1)}} - \frac{1}{\rho}\overline{p_c^{(1)}z_a^{(1)}} + \nu_0[2\overline{x_a^{(1)}x_{laa}^{(1)}} \\ + 2\overline{z_c^{(1)}x_{lcc}^{(1)}} + 2\overline{z_a^{(1)}x_{lac}^{(1)}} + 2\overline{x_c^{(1)}x_{lac}^{(1)}} \\ + \overline{x_{la}^{(1)}\nabla_L^2 x^{(1)}} + \overline{x_{lc}^{(1)}\nabla_L^2 z^{(1)}}]\end{aligned} \tag{3.1}$$

$$(\nu_0 - \kappa u_* c)\bar{y}_{lcc}^{(2)} - \kappa u_*\bar{y}_{lc}^{(2)} - \bar{y}_{lt}^{(2)} - f\bar{x}_l^{(2)} = 0, \tag{3.2}$$

where the overbars, as before, denote average over one wave cycle and $\nabla_L^2 = \partial^2/\partial a^2 + \partial^2/\partial c^2$. Furthermore, we have assumed that the mean current and mean pressure are independent of the coordinate a. Here, and in the rest of the paper, real values are used for the variables in the nonlinear terms.

Under these circumstances the dynamic boundary condition involving the mean *horizontal* wind stress $\bar{\tau}_x$ ($=\epsilon^2\bar{\tau}_x^{(2)}$) acting at the sea surface may be written to $O(\epsilon^2)$:

$$\begin{aligned}\bar{\tau}_x^{(2)} = \overline{p^{(1)}z_a^{(1)}} + \rho\nu_0[\bar{x}_{lc}^{(2)} + \overline{x_{lc}^{(1)}x_a^{(1)}} - \overline{x_{la}^{(1)}x_c^{(1)}} \\ + \overline{z_{la}^{(1)}z_c^{(1)}} - \overline{z_{lc}^{(1)}z_a^{(1)}} - 2\overline{x_{la}^{(1)}z_a^{(1)}}],\end{aligned}$$

$$c = 0. \tag{3.3}$$

It sometimes proves convenient to separate $\bar{\tau}_x$ into two parts (Weber and Førland 1989):

$$\bar{\tau}_x = \bar{\tau} - \overline{\sigma z_a}, \quad c = 0, \tag{3.4}$$

correct to $O(\epsilon^2)$. Here $\bar{\tau}$ is the mean *tangential* shear stress along the sea surface. The quantity $-\overline{\sigma z_a}$ is often referred to as the form drag τ_w. It represents the momentum flux from the wind to ocean waves. In the form drag, the fluctuating air pressure will usually constitute the dominating part of the normal stress, so approximately, $\tau_w \approx \overline{pz_a}$.

By utilizing (2.9), that is, continuity of normal stresses across the surface, the form drag in (3.4) may be expressed in terms of water variables. Equations (3.3) and (3.4) can then be combined to yield

$$\bar{x}_{lc}^{(2)} = \frac{\bar{\tau}^{(2)}}{\rho \nu_0} - \overline{x_{lc}^{(1)} x_a^{(1)}} + \overline{x_{la}^{(1)} x_c^{(1)}} - \overline{z_{la}^{(1)} z_c^{(1)}} + \overline{3 x_{la}^{(1)} z_a^{(1)}}, \quad c = 0. \tag{3.5}$$

Assuming that there are no wind and no waves in the y direction, we obtain

$$\bar{y}_{lc}^{(2)} = 0, \quad c = 0. \tag{3.6}$$

Defining a mean drift velocity (u, v) by

$$(u, v) = \epsilon^2(\bar{x}_l^{(2)}, \bar{y}_l^{(2)}) \tag{3.7}$$

and introducing a complex drift velocity $W = u + iv$ (as usual in this kind of problem), Eqs. (3.1) and (3.2) reduce to

$$(\nu_0 - \kappa u_* c) W_{cc} - \kappa u_* W_c - W_t - ifW = 4\nu_0 \zeta_0^2 \omega k^3 \times \left[\left(1 - \frac{\beta \gamma^2}{\omega k^2} \right) e^{2kc} - \frac{\gamma^3}{k^3} e^{\gamma c} \{ (B_r + B_i) \cos \gamma c - (B_r - B_i) \sin \gamma c \} \right] e^{2\beta t}, \tag{3.8}$$

where higher-order terms in k/γ have been neglected. Furthermore, we have assumed that

$$\frac{\gamma}{k} |B| \ll 1. \tag{3.9}$$

This assumption will be verified a posteriori. To the same approximation, the boundary conditions (3.5) and (3.6) can be written:

$$W_c = T + 2\zeta_0^2 \omega k^2 \left(1 - \frac{\gamma^2}{k^2} B_r \right) e^{2\beta t}, \quad c = 0. \tag{3.10}$$

Here we have defined $T = \bar{\tau}/(\rho \nu_0)$, where $\bar{\tau}$ is the mean tangential shear stress to $O(\epsilon^2)$ from the air on the water surface. Furthermore, we require

$$W \to 0, \quad c \to -\infty. \tag{3.11}$$

The problem defined by Eqs. (3.8), (3.10), and (3.11) yields the mean drift current induced by wind and waves as a function of the eddy-viscosity distribution in the water, the mean tangential wind stress, the growth rate of the waves, and the normal (or tangential) fluctuating wind stress along the surface.

4. The mean flow

To illustrate the nature of the Lagrangian mean-drift solution, it may conveniently be split into four different parts:

$$W = W^{(T)} + W^{(S)} + W^{(v)} + W^{(E)}. \tag{4.1}$$

By definition:

- $W^{(T)}$ current driven by the external, mean tangential shear stress
- $W^{(S)}$ classic Stokes drift modified by wave growth or decay
- $W^{(v)}$ vorticity layer correction
- $W^{(E)}$ quasi-Eulerian, wave-induced drift current.

This subdivision is made to make our results resemble those usually obtained from the more traditional Eulerian approach; for example, Jenkins (1986).

We denote the differential operator associated with the left-hand side of (3.8) by L. Then, by definition,

$$L = \nu \frac{\partial^2}{\partial c^2} + \nu' \frac{\partial}{\partial c} - \frac{\partial}{\partial t} - if, \tag{4.2}$$

where $' = d/dc$. The contribution $W^{(T)}$ in (4.1) is then obtained from

$$L\{W^{(T)}\} = 0, \tag{4.3}$$

subject to

$$\left. \begin{aligned} W_c^{(T)} &= T, \quad c = 0, \quad t > 0 \\ W^{(T)} &\to 0, \quad c \to -\infty \end{aligned} \right\}. \tag{4.4}$$

Additionally, we impose the initial condition

$$W^{(T)}(t = 0) = 0. \tag{4.5}$$

For constant eddy viscosity (4.3)–(4.5) reduce to the classic Ekman problem solved by Fredholm (Ekman 1905). When $\nu_0 = 0$, that is, $\nu = -\kappa u_* c$ from (2.1), analytical solutions of (4.3) have been obtained by Madsen (1977). In the present paper (4.3) is solved numerically. Some of the results will be presented later in connection with the discussion of the wave-induced current.

The friction velocity u_* in the water is related to the mean momentum flux from the air to the water by the viscous shear stress. Hence, for purely temporally decaying surface waves in the absence of wind, the friction velocity should be zero. Defining

$$u_* = (\bar{\tau}/\rho)^{1/2}, \tag{4.6}$$

where $\bar{\tau}$ is the mean tangential shear stress acting at the water surface, the nonlinear computations by Weber and Førland (1990) for constant eddy viscosity in fact show that $\bar{\tau} = 0$ for such waves. In the forthcoming analysis, with an imposed mean wind, we shall use the definition (4.6) for the friction velocity in the water.

For the nonrotating Stokes part in (4.1), we take

$$W^{(S)} = \zeta_0^2 \omega k e^{2kc+2\beta t}, \quad (4.7)$$

that is, the classic Stokes drift (Stokes 1847) for deep-water waves modified by wave growth or wave attenuation.

The vorticity-layer correction $W^{(v)}$ in (4.1) is confined to the thin boundary layer adjacent to the surface. It is governed by the equation

$$L\{W^{(v)}\} = -4\nu_0 \zeta_0^2 \omega \gamma^3 e^{\gamma c} \times [(B_r + B_i)\cos\gamma c - (B_r - B_i)\sin\gamma c] e^{2\beta t}. \quad (4.8)$$

Due to the rapid variation in the vertical, the effect of time variation and rotation can be neglected in this equation. From (4.8) we then easily obtain a first integral:

$$(\nu_0 - \kappa u_* c) W_c^{(v)} = -4\nu_0 \zeta_0^2 \omega \gamma^2 e^{\gamma c}[B_r \cos\gamma c + B_i \sin\gamma c] e^{2\beta t}. \quad (4.9)$$

The equation for the quasi-Eulerian current $W^{(E)}$ is now readily obtained from (3.8). Utilizing (4.7) and (4.8), we find

$$L\{W^{(E)}\} = \zeta_0^2 \omega k[2k\kappa u_*(2kc + 1) + if] e^{2kc+2\beta t}. \quad (4.10)$$

Invoking (4.4), (4.7), and (4.9), the boundary conditions (3.10) and (3.11) yield for $W^{(E)}$:

$$W_c^{(E)} = 2\zeta_0^2 \omega \gamma^2 B_r e^{2\beta t}, \quad c = 0 \quad (4.11)$$

$$W^{(E)} \to 0, \quad c \to -\infty. \quad (4.12)$$

Below the thin vorticity layer, $W^{(E)}$ is equal to the total wave-induced current minus the inviscid Stokes drift [calculated for waves with amplitude $\zeta_0 \exp(\beta t)$]. Hence, $W^{(E)}$ corresponds closely to the Eulerian wave-induced mean velocity, although still expressed in Lagrangian coordinates. Accordingly, if the wave field in the (essentially) inviscid bulk of the fluid is equal to the Stokes drift at the onset of wave motion, the initial condition for $W^{(E)}$ can be written

$$W^{(E)}(t = 0) = 0. \quad (4.13)$$

Further integration of (4.9) yields that the magnitude of $W^{(v)}$, even at the surface, will be much less than unity. Hence, the wave-induced current is essentially represented by $W^{(E)} + W^{(S)}$. Let us for a moment neglect the variation of the eddy viscosity. The solution for the total wave-induced drift current can then be obtained directly from the results in Weber and Førland (1990). Defining the wave-induced drift by $W^{(w)} = W^{(S)} + W^{(E)}$, we find

$$W^{(w)} = \zeta_0^2 \omega k \Big[F e^{2kc+2\beta t} + 2k\nu_0^{1/2}\Big(1 - F + \frac{\gamma^2}{k^2} B_r\Big) \times e^{2\beta t} \int_0^t \frac{\exp((-2\beta - if)\xi - c^2/(4\nu_0\xi))d\xi}{(\pi\xi)^{1/2}} + 2k\nu_0^{1/2}(1 - F)e^{-if t} \times \int_0^\infty \frac{\exp(-\xi t)\cos(c\xi^{1/2}/\nu_0^{1/2})d\xi}{\pi\xi^{1/2}(\xi + 4k^2\nu_0)} \Big], \quad (4.14)$$

where

$$F = \left[1 - \frac{if}{4k^2\nu_0(1 - \beta\gamma^2/\omega k^2)}\right]^{-1}. \quad (4.15)$$

Here the growth rate β and the parameter B_r are unspecified. The only restrictions imposed on the solution (4.14), apart from the assumption of a constant eddy viscosity, are given by the inequalities (2.14) and (3.9).

It is also worth pointing out that our analysis for growing/decaying waves yields a nonzero, net mass transport even if the viscosity in the water is completely neglected! Disregarding water viscosity altogether, we obtain from (3.8) for the wave-drift current

$$W_t^{(w)} + ifW^{(w)} = 2\beta\zeta_0^2 \omega k e^{2kc+2\beta t}, \quad (4.16)$$

where β is obtained entirely from the wave-modulated motion in the air. For $\beta = 0$, this result conforms to those obtained earlier by Ursell (1950) and Hasselmann (1970) of no net transport in an inviscid, rotating ocean.

We note from (4.16) that for large growth/decay rates ($|\beta| \gg f$) the solution essentially yields the classic Stokes drift in the direction of the waves. For small growth/decay rates the net drift is essentially perpendicular to the wave propagation direction and proportional to $-\beta/f$. The reason for this net mass transport by growing/decaying waves in an inviscid, rotating ocean is the work of the fluctuating air pressure at the sea surface.

5. Estimation of the unknown parameters

The variable wind-stress distribution at the surface and the growth rate β of the waves could in principle be obtained from field measurements. This, however, is an extremely difficult task. Apart from the purely technical problems, observed growth rates are likely to have been influenced by energy transfer between various components of the wave spectrum. This effect is not included in the present theory. Also, for stronger winds, the occurrence of whitecapping will influence the surface-stress distribution (Banner 1990), as well as convert mean momentum directly from the waves to the mean current (Mitsuyasu 1985). For a further discussion of this topic, the reader is referred to Phillips (1977, 1985). Despite these difficulties, we shall, to some extent, rely on empirical relations obtained from observational data (Plant 1982; Mitsuyasu and Honda 1982) to quantify the wave growth.

Alternatively, the surface-stress distribution and the wave growth may be determined theoretically. This is by no means simpler, mainly owing to the turbulent nature of the airflow above the water. Hence, we have

to be content with simplified models for the flow structure. In Miles' (1957) celebrated model for wave growth due to shear instability, the presence of turbulence only manifests itself through the shape of the wind profile. Recent experience from ocean wave modeling, however, suggests that the turbulent Reynolds stress may play a dominant part in the wave generation process (Chalikov and Makin 1990). In that case we may apply the results from the asymptotic analyses by Knight (1977) and Jacobs (1987) to obtain the growth rate and the turbulent stress at the surface. These studies apply in essence an eddy assumption for the turbulent Reynolds stress. This leads to a linearly increasing eddy viscosity coefficient in the logarithmic wind regime, as one would expect from mixing-length theory.

Although attacking the problem in somewhat different ways, the main results of the asymptotic analyses by Knight (1977) and Jacobs (1987) are essentially the same. In our notation, Knight's growth rate may be written:

$$\beta = \kappa U_* ks\left[\frac{U-C}{C}\right] - \frac{\omega k^2}{\gamma^2}. \tag{5.1}$$

Here U is the wind speed at height k^{-1} and $C = \omega/k$ the phase speed of the waves. The frequency in this approximation is given by $\omega = \omega_0 = (gk)^{1/2}$. Furthermore, $s = \rho_a/\rho$ is the density of air ρ_a relative to that of water, and U_* is the friction velocity in the air.

The real part of the amplitude of the normal stress, valid outside the viscous sublayer in the air, may be obtained from Knight's and Jacobs' analyses as

$$\sigma_{1r} = -2\kappa U_* ks\left[\frac{U-C}{C}\right]. \tag{5.2}$$

We assume that the normal stress is continuous and practically constant through the very thin sublayer. Hence, the expression (5.2) can be applied at the air–water interface, given by $c = 0$. Utilizing the results (5.1) and (5.2), Eq. (2.13) then yields that the imaginary part of the tangential stress amplitude τ_1 at the surface vanishes in this approximation. This result is in accordance with (2.18). Hence, from (2.12), we obtain for the real part of the parameter B, featuring in the boundary condition (4.11) for the quasi-Eulerian wave-drift current,

$$B_r = k^2/\gamma^2 = 2k^2\nu_0/\omega. \tag{5.3}$$

For the "background" turbulence associated with ν_0, we use the result from Bye (1988) for the near-surface viscosity:

$$\nu_0 = \frac{1}{s}\frac{\kappa u_*^3}{2Kg}, \tag{5.4}$$

where u_* is the friction velocity in the water and K is obtained from the wave spectrum. Bye suggests $K = 0.35$.

From the logarithmic wind profile we obtain for the wind speed at height k^{-1}, appearing in (5.1) and (5.2),

$$U = \frac{U_*}{\kappa}\ln\left[\frac{1}{kz_0}\right], \tag{5.5}$$

where z_0 is the roughness length in the air. For aerodynamically rough flow we may apply Charnock's formula for z_0 (Charnock 1955):

$$z_0 = \frac{AU_*^2}{g}, \tag{5.6}$$

where $A = 0.0185$ for a fully developed sea (Wu 1982). Actually, the surface roughness is a function of the sea state; see for example the review article by Donelan (1990). The Charnock relation used here will only give consistent results for a saturated sea, that is, for large wave age. For young sea, the roughness is somewhat larger than that given by (5.6), as seen from Fig. 3 in the recent paper by Maat et al. (1991). For the rather idealized situation considered in the present paper, however, where we look at individual wave components before they break, it is sufficient to use (5.6) for parameterizing the roughness length.

As we now have formulated the problem, the various parameters are, for a given wavenumber, only functions of the friction velocities in the water and in the air. The latter may, in turn, through the traditional introduction of a drag coefficient, be connected to the wind speed at a prescribed height, usually taken to be 10 m. Furthermore, from continuity of mean stresses at the air–water interface, we must require $U_* = u_*/s^{1/2}$. Of particular interest here is the nondimensional growth rate β/ω. For given U_* this will vary with the wavenumber k or the wavelength $\lambda = 2\pi/k$. Denoting the wavelength that maximizes β by λ_m, we may obtain λ_m and $\beta = \beta(\lambda_m; U_*)$ numerically from (5.1), using (5.4)–(5.6). The results are summarized in Table 1. Utilizing the relations $\omega = (2\pi g/\lambda_m)^{1/2}$ and $C = (g\lambda_m/2\pi)^{1/2}$, these results can be combined to yield

$$\frac{\beta}{\omega} = 1.2\times 10^{-3}\frac{U_*^2}{C^2}. \tag{5.7}$$

In his analysis of the wave-growth problem, Jacobs (1987) finds that the meteorological data from the field experiments by Snyder et al. (1981) do suggest a much smaller value for the constant A in Charnock's relation (5.6). As an appropriate value for the initial phases of wave growth, Jacobs assumes $A = 0.0028$ (in our notation). This will, for a given value of k and U_*, in-

TABLE 1. Maximum growth rate from (5.1) as function of friction velocity in the air.

U_* (m s^{-1})	0.1	0.2	0.3	0.5	1.
λ_m (m)	0.4	1.7	3.7	10.4	41.6
β (10^{-4} s^{-1})	2.2	1.2	0.7	0.4	0.2

crease the wind speed U and, hence, the growth rate β. Using Jacobs' value for A, we find from (5.1), by inserting for the fastest-growing wave, that the coefficient in (5.7) increases by a factor of 2.

In fact, analyses of experimental data indicate an empirical relationship between the dimensionless growth rate β/ω, the phase speed $C = \omega/k$, and the friction velocity U_* of the form (5.7); that is,

$$\frac{\beta}{\omega} = \alpha_* \frac{U_*^2}{C^2}. \tag{5.8}$$

From Plant's (1982) survey of field and laboratory observations we find $\alpha_* = (2 \pm 1) \times 10^{-2}$ in our notation. Similarly, from the model tank experiments by Mitsuyasu and Honda (1982), we obtain $\alpha_* = 2.7 \times 10^{-2}$. It is worth noting that the values for α_* stated here are about one order of magnitude larger than those obtained from the theoretical assessment (5.7). In this context it is fair to mention that the value of α_* reported by Jacobs (1987) actually was larger than twice that of (5.7). This was due to the neglect of friction in the water; that is, the last term on the right-hand side of (5.1) is missing from Jacobs' analysis.

For the wave speed corresponding to maximum growth we find from the computations leading to (5.7) that

$$C = 8.1 U_*. \tag{5.9}$$

This fits quite well with observational data, which suggest $C \sim 10U_*$ for the most rapidly growing waves (Jacobs 1987). By combining the results (5.7) and (5.9), we realize the fact that the ratio β/ω for the fastest growing wave is constant.

The discrepancy displayed here between theoretical and observed values of the growth rates leads one to suspect that finite-amplitude effects may be important. Hence, it may happen that a simple eddy-viscosity model for the air turbulence is insufficient at modeling the turbulent Reynolds stress in the flow over finite-amplitude waves. In addition, as mentioned in the beginning of this paragraph, it is difficult to exclude from field data the wave growth due to the nonlinear transfer of energy from various other components of the wave spectrum.

6. Discussion of the eddy viscosity assumption

In the present approach we have chosen to use an eddy viscosity assumption for the turbulent Reynolds stress. This is, of course, a rather crude approximation, but unfortunately difficult to avoid if one wishes to obtain analytical solutions of problems involving turbulent motion.

It is worth noting here that there is a fundamental difference between the flow in the air and the flow in the water. In the air, the turbulent wind dominates the motion. The gravity waves that are generated at the air–sea interface induce motions that are small compared to the mean wind. It may therefore be justified to assume a complete analogy between the Newtonian viscosity and the spatially varying eddy viscosity in modeling the air stress tensor (Jacobs 1987). In the water the situation is different. Here the waves constitute the dominant contribution to the velocity field, while the surface stress- and wave-induced mean currents are smaller by an order of magnitude, or so. The nearly orbital motion associated with the primary wave field is not really turbulent but superimposed on a turbulent field generated by wind stress, wave breaking, buoyancy-driven convection, etc. in the surface layer. The waves themselves are only weakly influenced by this turbulence. We have therefore chosen not to include the gradients of the pure wave motion in the dominating parts of the turbulent Reynolds stress, being proportional to the depth-varying eddy viscosity. This led to a stress tensor whose divergence is given by (2.2).

In this context it may be of interest to discuss some consequences of applying a stress tensor in the water similar to that in the air. In Eulerian form we may then write

$$\frac{1}{\rho}\frac{\partial}{\partial x_j} P_{\text{turb}}^{(ij)} = \nu \nabla^2 u_i + \frac{\partial \nu}{\partial x_j}\left[\frac{\partial u_j}{\partial x_i} + \frac{\partial u_i}{\partial x_j}\right] - \frac{2}{3}\frac{\partial}{\partial x_i} K_{\text{turb}}, \tag{6.1}$$

where u_i ($i = 1, 2, 3$) is the total water velocity (including waves) averaged over a period that is large compared with the typical period of the turbulent motion but much smaller than the wave period. As in (2.2), K_{turb} is the kinetic energy per unit mass of the turbulent fluctuations.

When applying (6.1), it is quite simple to show that the Lagrangian wave problem to $O(\epsilon)$ may be separated in the familiar way (Lamb 1932):

$$\left.\begin{aligned} x_l^{(1)} &= -\varphi_a - \psi_c \\ z_l^{(1)} &= -\varphi_c + \psi_a \end{aligned}\right\}, \tag{6.2}$$

where $\nabla_L^2 \varphi = 0$. For the particular case of a *linearly* varying eddy viscosity, we find for the vorticity part of the wave field,

$$\psi_t - \nu \nabla_L^2 \psi = 0. \tag{6.3}$$

This is the same form as that obtained by Lamb for constant viscosity. Here, however, $\nu = \nu_0 - \kappa u_* c$. Furthermore, the fluctuating pressure may be written

$$\frac{p^{(1)}}{\rho} = -g z^{(1)} + \varphi_t + 2\nu_c z_t^{(1)}, \tag{6.4}$$

where we note the extra term on the right-hand side owing to the variation of ν. It should be emphasized that (6.2)–(6.4) constitute an exact solution of the nonrotating, linear system of equations in the water when ν_c is constant.

Utilizing the fact that the normal stress must be continuous across the surface, we find for the leading term in the form drag, defined by (3.4):

$$\tau_w \approx \epsilon^2 \overline{p^{(1)} z_a^{(1)}}, \quad c = 0. \tag{6.5}$$

Here $p^{(1)}$ is given by (6.4). We observe that the main contribution to τ_w is obtained from the turbulent Reynolds stress part of the pressure. The leading term can then be written

$$\tau_w \approx 2\rho\epsilon^2 \nu_c \overline{z_t^{(1)} z_a^{(1)}}|_{c=0} = \rho\kappa u_* C\delta^2, \tag{6.6}$$

where the potential part of $z^{(1)}$ is obtained from (2.4) and $\delta = k\zeta_0 \exp(\beta t)$ is the instantaneous wave slope.

Let us consider two different cases: (i) gently sloping, growing waves ($\delta \sim 0.15$) and (ii) a fully developed sea ($\delta \sim 0.3$). In the first case we assume that $C \sim 10U_*$ for the speed of the fastest-growing wave (Jacobs 1987). For a fully developed sea the phase speed corresponding to the peak of the wave spectrum is approximately equal to the wind speed U_{10} at 10-m height (Phillips 1977). Alternatively, $C \sim U_* c_{10}^{-1/2}$, where c_{10} is the drag coefficient at 10 m ($c_{10} \sim 1.5 \times 10^{-3}$). From (6.6), with $U_*^2 = u_*^2/s$, we then obtain for the cases (i) and (ii) that $\tau_w/\tau_0 \sim 2.6$ and $\tau_w/\tau_0 \sim 27$, respectively. Here $\tau_0 = \rho_a U_*^2$ is the total horizontal momentum flux in the air. Since τ_w/τ_0 never can exceed unity, the results derived here do not make sense. Accordingly, the Reynolds stress in the ocean cannot be modeled by a linearly increasing eddy viscosity (proportional to κu_*) combined with the shear of the primary wave field.

Let us now for a moment return to our model (2.2) for the Reynolds stress. The form drag τ_w may be obtained from (2.4) and (2.9) as

$$\tau_w = -\epsilon^2 \overline{\sigma^{(1)} z_a^{(1)}} = \rho\left(\frac{\beta}{\omega} + \frac{1}{2} B_r + \frac{1}{2}\frac{k^2}{\gamma^2}\right) C^2\delta^2, \tag{6.7}$$

where again $\delta = k\zeta_0 \exp(\beta t)$. Utilizing the theoretical values (5.1) and (5.2) from Knight's (1977) analysis, (6.7) reduces to

$$\tau_w = \rho_a \kappa U_* (U - C)\delta^2. \tag{6.8}$$

From (5.1) and (5.4)–(5.6) we find $U \sim 20U_*$ and $C \sim 10U_*$ for the fastest-growing waves. Hence, with $\delta \sim 0.15$, we obtain $\tau_w/\tau_0 \sim 0.1$ from (6.8), which is a perfectly reasonable result.

For a fully developed spectrum (old sea), Phillips (1977) concludes that $\tau_w \ll \tau_0$. For younger, rougher sea, however, τ_w/τ_0 may be close to unity (Janssen 1989). Similarly, from laboratory experiments, Banner (1990) finds that most of the observed total stress enhancement associated with wave breaking is reflected in a correspondingly large increase in the form drag.

Applying empirical growth rates in our theoretical results, the β/ω term will dominate in (6.7). Using the empirical relation (5.8), we find in this case:

$$\tau_w = \rho\alpha_* U_*^2 \delta^2. \tag{6.9}$$

Now taking $\delta \sim 0.15$ and $\alpha_* \sim 0.01$, we obtain $\tau_w/\tau_0 \sim 0.2$. It is therefore reassuring to find that our eddy viscosity assumption yields results that do not violate the basic physics of the problem.

7. Volume fluxes in the upper ocean

Many classic results concerning the general ocean circulation are formulated in terms of vertically integrated currents, that is, volume fluxes per unit horizontal length. As far as the upper, mixed layer of the ocean is concerned, one might infer from earlier analyses, like those of Bye (1967) and Kenyon (1969), that the correct volume flux is obtained by *adding* the wave-induced flux associated with the classic, steady Stokes drift to that obtained from the wind stress (the Ekman transport). As will be demonstrated here, this is generally not the case. To prove this point, it is advantageous to use the previous partition (4.1) of the total, Lagrangian mean current.

We define a complex volume flux per unit length by

$$Q = \int_{-\infty}^{0} W dc. \tag{7.1}$$

Integrating (4.3) and using (4.4), we obtain immediately that

$$\frac{d}{dt} Q^{(T)} + ifQ^{(T)} = \bar{\tau}/\rho = u_*^2. \tag{7.2}$$

This is the equation for the traditional Ekman transport, driven by the mean tangential shear stress at the surface.

The classic Stokes drift $W^{(S)}$ from (4.7) yields a nonzero contribution in the direction of the waves

$$Q^{(S)} = \tfrac{1}{2}\omega\zeta^2, \tag{7.3}$$

where we again have used $\zeta = \zeta_0 \exp(\beta t)$ for the instantaneous wave amplitude.

For the quasi-Eulerian contribution, we find from (4.10)–(4.12)

$$\frac{d}{dt} Q^{(E)} + ifQ^{(E)} = \left(-\tfrac{1}{2} if\omega + \omega^2 B_r\right)\zeta^2 = -ifQ^{(S)} + \omega^2 B_r \zeta^2, \tag{7.4}$$

where $Q^{(S)}$ is defined by (7.3).

The volume flux due to the vorticity-layer correction $W^{(v)}$ is negligibly small. Hence, the total wave-induced transport $Q^{(w)}$ is given by $Q^{(w)} = Q^{(S)} + Q^{(E)}$. Equations (7.3) and (7.4) then yield

$$\frac{d}{dt} Q^{(w)} + ifQ^{(W)} = \left(B_r + \frac{\beta}{\omega}\right)\omega^2\zeta^2. \tag{7.5}$$

We thus notice that the contribution (7.3) from the classic Stokes drift to the total wave-induced flux is

canceled by an equal, and opposite, quasi-Eulerian flux term in (7.4). The only remaining Stokes drift contribution to (7.5) is the second term on the right-hand side, which is the *time derivative* of $Q^{(S)}$. This result could also have been obtained directly by integrating (3.8) and using the boundary condition (3.10). That approach, however, would not have revealed explicitly the fate of the disputed, steady Stokes-induced volume flux. By integrating (7.5) we obtain

$$Q^{(w)} = \left[\frac{\beta/\omega + B_r}{2\beta + if}\right]\omega^2\zeta^2 + Q_i e^{-ift}, \qquad (7.6)$$

where the last term on the right-hand side represents purely inertial motion. The amplitude Q_i is determined by the initial conditions. We notice from (7.6) that the magnitude and direction of this wave-induced flux crucially depend on the ratio $|\beta|/f$.

For slowly growing/decaying waves ($|\beta| \ll f$) we find from (7.6) for the noninertial part Q_0 of the volume flux:

$$Q_0 \approx -\frac{2i\beta}{f}(1 + \omega B_r/\beta)Q^{(S)}. \qquad (7.7)$$

This flux component is directed perpendicular to the wind and wave direction. Furthermore, it is obvious that Q_0 is much smaller than the Ekman flux u_*^2/f.

For rapidly growing/decaying waves ($|\beta| \gg f$) the situation is quite different. Now we obtain from (7.6) that

$$Q_0 \approx (1 + \omega B_r/\beta)Q^{(S)}. \qquad (7.8)$$

In this case we see that the noninertial component of the wave-induced flux is directed along the wind and wave direction. Utilizing the empirical relationships stated in section 5 for rapidly growing waves, we find that the contribution (7.8) may be of the same order of magnitude as the Ekman flux (but directed along the wind) when the waves are steep. One can speculate about what will happen when the rapidly growing waves become so steep that they break. Then, of course, our calculations are no longer valid. Physically, however, there must be some sort of balance between energy input from the wind and energy loss due to repeated wave breaking. How to model this process is far from clear at the moment.

8. Numerical results and discussions

It is not the aim of the present paper to study the complicated buildup of a certain sea state from infinitesimal, fast-growing wind waves. Instead, we focus on the development of the nonlinear drift current in the ocean. For this purpose we consider regular, finite-amplitude monochromatic waves influenced by local winds. From Knight's and Jacobs' simplified analyses for the turbulent motion in the air, the modulated wave amplitude is obtained; see Eq. (5.1). We consider drift currents associated with damped as well as growing waves. This is obtained here by letting the waves travel against or along the wind direction, respectively.

a. *Wind-driven current*

We first consider the wind-stress part $W^{(T)}$ of the mean current. For given friction velocity this contribution is readily obtained by integrating (4.3) numerically. The result for a suddenly imposed shear stress in the x direction is presented in Fig. 1. We have taken $u_* = 0.016$ m s^{-1} in this example, and the computed current is nondimensionalized by u_*. Here, and in all the computations presented in section 8, we have used $f = 1.2 \times 10^{-4}$ s^{-1}. Hodographs are plotted at depths 0, 1, 5, 20, and 50 m, respectively (solid lines). The black dots and numbers on the graphs denote time in pendulum hours after the onset of motion, and the

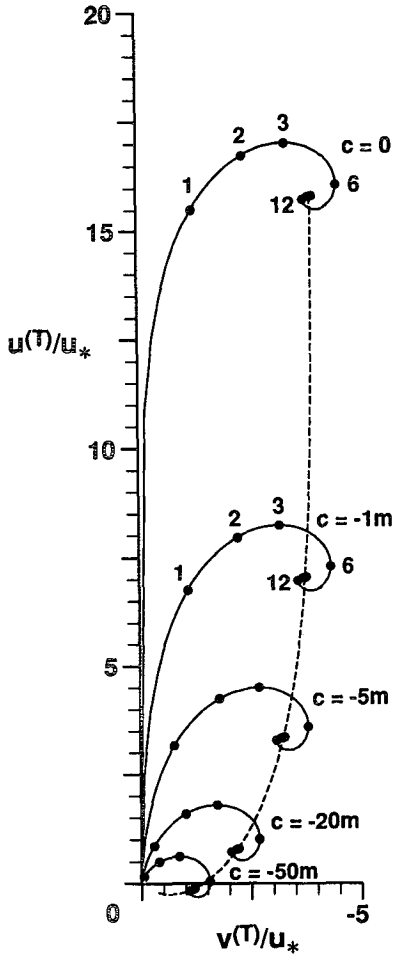

FIG. 1. Hodographs of the dimensionless wind-driven current $W^{(T)}/u_*$ from (4.3) at depths 0, 1, 5, 20, and 50 m, respectively (solid lines). Here, and in the following figures, the numbered black dots denote evolution time in pendulum hours. The broken line depicts the depth-varying steady-state solution. In this example $u_* = 0.016$ m s^{-1}.

broken line represents the steady-state hodograph (the Ekman spiral). The results are very similar to those obtained by Madsen (1977) and Jenkins (1987). In particular we note that the present eddy viscosity distribution with depth yields a surface current that is aligned more closely along the wind direction than Ekman's 45 deg. In this example the deflection angle is about 14 deg. Furthermore, if we assume a drag coefficient of 1.5×10^{-3}, the magnitude of the surface current is here about 2% of the wind speed at 10-m height. It is also obvious from the figure that an eddy-viscosity distribution of the form (2.1) effectively enhances the damping of the inertial oscillations that are part of the transient drift solution.

b. *Temporally damped waves*

Concerning the wave-induced part of the total drift current, we first consider temporally damped waves. From (5.1) damping occurs for all wavelengths when $U < 0$, that is, when the waves travel against the wind. In general, it is seen that the waves are damped very efficiently by adverse winds. For a wavelength $\lambda = 100$ m and a friction velocity $u_* = 0.016$ m s^{-1}, (5.1) yields $\beta = -3 \times 10^{-5}$ s^{-1}. The contribution to β from the oceanic viscosity [second term in (5.1)] is here much smaller than the wind term. Nonlinearly, this increased damping will lead to smaller drift currents.

The total wave-induced current, $W^{(w)} = W^{(S)} + W^{(E)}$, is obtained by adding (4.7) to the numerical solution of (4.10)–(4.12). The result for the surface current, scaled by u_*, is displayed in Fig. 2 (solid line). The initial wave amplitude ζ_0 was taken to be 1 m. In order to emphasize the effect of the variable eddy viscosity, we have also depicted the equivalent wave drift current from (4.14) for constant eddy viscosity (broken line). The equivalent case (same β) has a constant, effective eddy viscosity $\nu_{\text{eff}} = -\beta/(2k^2)$. Furthermore, $B_r = 2k^2\nu_{\text{eff}}/\omega$. We note from the figure that the present eddy-viscosity variation leads to a more rapid decrease of the surface current, as well as to a stronger suppression of the inertial part of the mean motion. Also, we find that the surface current is more aligned along the direction of applied forcing (here, the wave propagation direction) than for constant eddy viscosity. This is quite similar to what one finds for the wind-stress driven part of the problem.

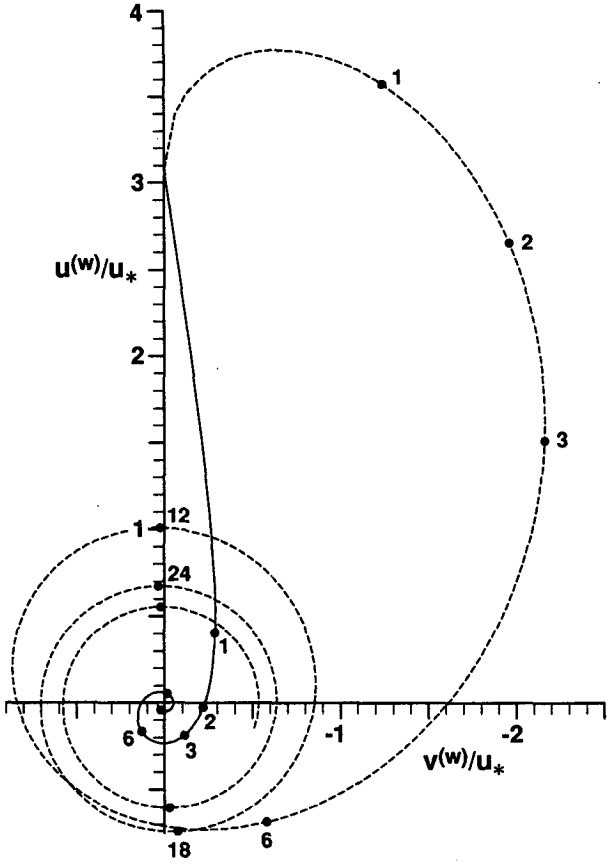

FIG. 2. Hodographs of the dimensionless wave-induced surface current $W^{(w)}/u_*$ from (4.7) and (4.10) (solid line) for temporally damped waves caused by adverse winds. Here $\lambda = 100$ m and $u_* = 0.016$ m s^{-1}. The broken line represents the equivalent surface current when the eddy viscosity does not vary with depth; see the text for details.

c. *Spatially damped waves*

One application of the present theory appears to be the damping of swell. Swell consists of nearly monochromatic waves propagating away from a distant generation (storm) area. Such waves may travel over large distances without much loss of energy. When they enter an area of local winds, however, a change of wave amplitude may occur. In the JONSWAP experiment, Hasselmann et al. (1973) found a pronounced damping of swell. Friction in the water, and in particular bottom friction, could not explain this decay in a consistent manner.

The fractional loss of swell energy from the outermost station to the shore was reported to lie in the range 0.7–0.2. Judging from the position of stations measuring at times when the wind was offshore, this yields a typical exponential attenuation coefficient α for the wave amplitude of order -10^{-5} m^{-1}. Theoretically, the relation between temporal and spatial growth/decay may be written

$$\alpha = \beta/C_g, \tag{8.1}$$

where C_g is the group velocity (Gaster 1962). From the observations by Hasselmann et al. (1973), we find a typical swell period of about 10 sec. Taking the average water depth to be 20 m, this yields phase and group velocities of 12.2 and 9.1 m s^{-1}, respectively. In order to give attenuation rates comparable to those derived from the experiments, the present theory requires adverse winds of about 16 m s^{-1} ($u_* = 0.025$ m s^{-1}). However, the wind speeds during the JON-

SWAP experiment were usually much lower than this, which may explain why the observed damping did not correlate particularly well with the wind speed (Hasselmann et al. 1973).

The current in the spatially attenuated case will be obtained for deep-water waves only. We utilize the fact that the vorticity-layer correction $W^{(v)}$ must be of the form (4.8), with spatial decay substituted for temporal decay. The governing equation for the wave drift will now contain a nonzero mean pressure gradient in the wave-propagation direction, plus a small vertical mean velocity from the equation of continuity; see Weber and Førland (1990). For the wave-induced current $W^{(w)} = W^{(S)} + W^{(E)}$ we now obtain

$$L\{W^{(w)}\} = 4\nu_0\zeta_0^2\omega k^3 e^{2\alpha a + 2kc}, \quad a \geq 0, \quad (8.2)$$

subject to

$$W_c^{(w)} = 2\zeta_0^2\omega k^2\left(1 + \frac{\gamma^2}{k^2}B_r\right)e^{2\alpha a}, \quad c = 0 \quad (8.3)$$

and

$$W^{(w)} \to 0, \quad c \to -\infty. \quad (8.4)$$

Here we have assumed that $|\partial^2/\partial c^2| \gg |\partial^2/\partial a^2|$ everywhere. Furthermore, the initial condition becomes

$$W^{(w)}(t = 0) = \zeta_0^2\omega k e^{2\alpha a + 2kc}. \quad (8.5)$$

As a theoretical example of pronounced wind damping ($\alpha < 0$), we consider an extreme case where $u_* = 0.025$ m s^{-1}, that is, an adverse wind $U_{10} \sim 16$ m s^{-1}. For incoming swell with a period of 10 sec and an initial wave amplitude $\zeta_0 = 1$ m, (8.2)–(8.5) are solved numerically. The results for $c = 0$ and $c = -15.6$ m, evaluated at $a = 0$ and nondimensionalized by the corresponding u_*, are displayed in Fig. 3. The development of the wave-induced current is very similar to that found in Fig. 2 for the temporally damped case. Now, however, we obtain a steady-state solution as $t \to \infty$. In this example the steady surface current is about 6% of the initial Stokes drift and is directed nearly in the same direction.

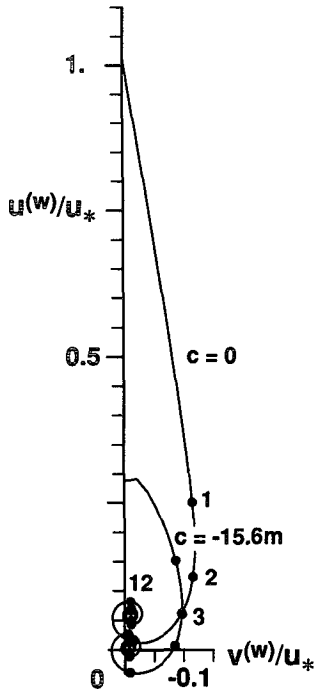

FIG. 3. Hodographs of the dimensionless wave-induced current $W^{(w)}/u_*$ from (8.2) at depths 0 and 15.6 m, respectively, for spatially damped waves where the damping is caused by adverse winds. Here the wave period $T = 10$ s and $u_* = 0.025$ m s^{-1}.

d. Growing waves

When the waves travel in the direction of the wind, wave growth may occur; see Table 1. For the wind and wave parameters $u_* = 0.025$ m s^{-1} and $\lambda = 100$ m, we now obtain $\beta = 2.6 \times 10^{-6}$ s^{-1} from (5.1). This represents slowly growing waves (e-folding time $1/\beta$ of about 4½ days). Figure 4 displays the development of the wave-induced current $W^{(w)} = W^{(S)} + W^{(E)}$ from (4.7) and (4.10) when $\zeta_0 = 1$ m. The results are scaled by u_*, and hodographs are depicted at $c = 0$ and $c = -10$ m. We again note a rather rapid decrease of the current with time at the early stages of the motion. This is quite similar to what was found for damped waves; see Figs. 2 and 3. This is because the exponential time dependence in the forcing term is close to unity for small times whether β is positive or negative. The quasi-Eulerian part of the solution is dominated by the contribution from the variable eddy-viscosity term on the right-hand side of (4.10). This yields a value for $W^{(E)}$ that essentially opposes the Stokes drift (4.7) at this stage of the motion. As time progresses, the Coriolis force becomes increasingly important and halts further decay of the drift current. At even larger times the inertial oscillations tend to vanish. The drift current is now dominated by the effect of growing wave amplitude and a balance between Coriolis and frictional forces. We note the pronounced veering with depth of the current for larger times, as seen from the hodograph at 10-m depth.

Rapidly growing waves are relatively short compared to those that usually constitute the dominant part of observed wave spectra. For growing waves we have from (5.9) that $C \sim 10U_*$, while for the peak of the spectrum one obtains approximately $C \sim U_{10} \sim 30U_*$ (Phillips 1977). As these short waves continue to grow the wave steepness δ will ultimately reach a point where breaking starts, and whitecaps may form. It is pertinent here to remind ourselves of the fact that the present approximation for the drift current presupposes a sufficiently small value of δ. Furthermore, description of the wave breaking process is definitely outside the scope (and ability) of the present approach. Despite this, we shall use our results up to the point where breaking may start. A single wave is assumed to break when δ

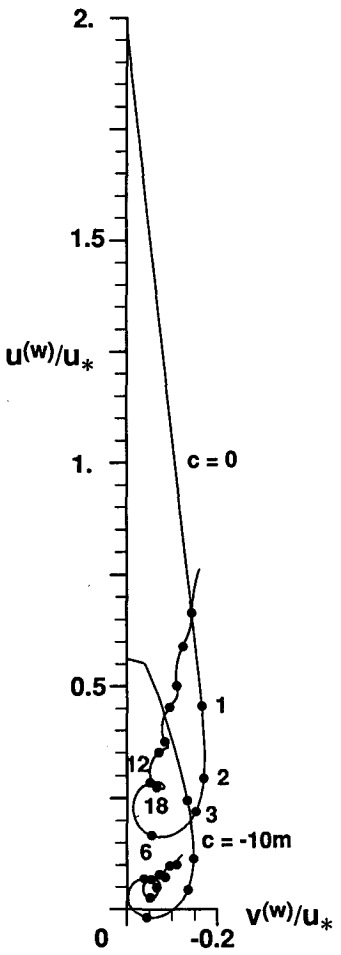

FIG. 4. Hodographs of the dimensionless wave-induced current $W^{(w)}/u_*$ from (4.7) and (4.10) at depths 0 and 10 m, respectively, for growing waves with wavelength $\lambda = 100$ m. Here $u_* = 0.025$ m s^{-1}.

$> \delta_c$. We here take $\delta_c = 0.3$, corresponding to a fully saturated sea.

In Fig. 5 we have displayed the computed drift current induced by a rapidly growing wave component. We have chosen $u_* = 0.016$ m s^{-1}; that is, a wind $U_{10} \sim 11.5$ m s^{-1}. For this friction velocity, we find from (5.1) that the fastest growing wave has a wavelength of 8.5 m. The computation of the wave-induced current has been continued until the wave steepness reaches the critical value. Taking the initial wave amplitude to be $1/10$ of the amplitude at $\delta = \delta_c$, the approximate breaking condition is reached after about 13 hours in this example. The plot shows hodographs of the non-dimensional wave-induced current $(u^{(w)}/u_*, v^{(w)}/u_*)$ at depths 0, 0.4, 1.7, and 8.5 m, respectively. We note the fact that the rapid wave growth and the relatively short time scale of this computation effectively prevents inertial oscillations from appearing in the drift solution. This can be seen by comparison with the current depicted in Fig. 4, which is induced by waves that grow more slowly. Also for rapidly growing waves, however, the effect of the earth's rotation is of importance for the development of the drift current. This is clearly seen from the veering to the right with depth of the current depicted in Fig. 5.

It should also be noted that the variation of the drift current at small times; that is, a decrease in the early stages of motion, as seen in Fig. 4, is also present here. Due to the velocity scaling in the plot, however, this tendency is not visible in Fig. 5.

It is of considerable interest to investigate how the wave-induced current varies with the friction velocity. For all possible growing waves at a given value of u_*, our description of the problem will break down when the steepness of a particular wave component reaches the critical value δ_c. We shall here assume that this particular wave component is that of maximum growth rate, although, depending on the initial conditions, the

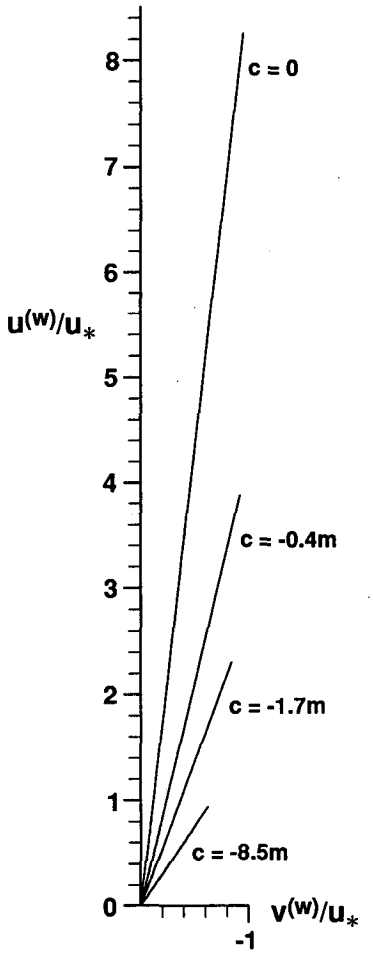

FIG. 5. Hodographs of the dimensionless wave-induced current $W^{(w)}/u_*$ from (4.7) and (4.10) at depths 0, 0.4, 1.7, and 8.5 m, respectively, for growing waves with wavelength $\lambda = 8.5$ m. Here $u_* = 0.016$ m s^{-1}. The computations of the hodographs are terminated after about 13 hours.

condition $\delta = \delta_c$ may theoretically be realized first for waves with slower growth rates. We note from Table 1 that increasing friction velocity implies that the maximum growth rate decreases and that this maximum occurs for increasingly longer waves.

In Fig. 6 we have plotted the wave-induced surface current as function of u_*. The displayed values are those obtained at the time when $\delta = \delta_c = 0.3$ for the fastest growing wave component. We note from the figure that the magnitude of the nondimensional wave drift current $|W^{(w)}|/u_*$ varies little with u_*. The deflection angle θ to the right of the wind and wave direction is small and lies between 2 and 10 deg. Typically, for $u_* = 0.016$ m s^{-1} we see that $|W^{(w)}| = 0.14$ m s^{-1}. Together with the direct wind-induced surface current displayed in Fig. 1, we find that the total wind- and wave-induced surface drift current in this example is about 3.5% of the wind speed at 10-m height and is directed 11.4 deg to the right of the wind direction. This result agrees very well with the usual "rule of the thumb" for observed wind- and wave-driven ocean surface currents. One should remember, however, that the wave-induced current here is only computed for the dominant wave component up to the point where breaking is likely to occur. At later stages the wave amplitude may equilibrate in an average sense. In this regime the energy balance is basically between energy input from the wind and dissipation due to wave breaking. Formally, one cannot infer from the present analysis what will really happen in the equilibrium range. However, since the wave amplitude virtually becomes constant when averaged over many breaking events (and close to that first attained at $\delta = \delta_c$) we think that the results displayed in Fig. 6 may still have some relevance. The present analysis is valid for constant wind. In a real situation the wind will vary in strength as well as in direction. This will influence the development of the induced ocean current.

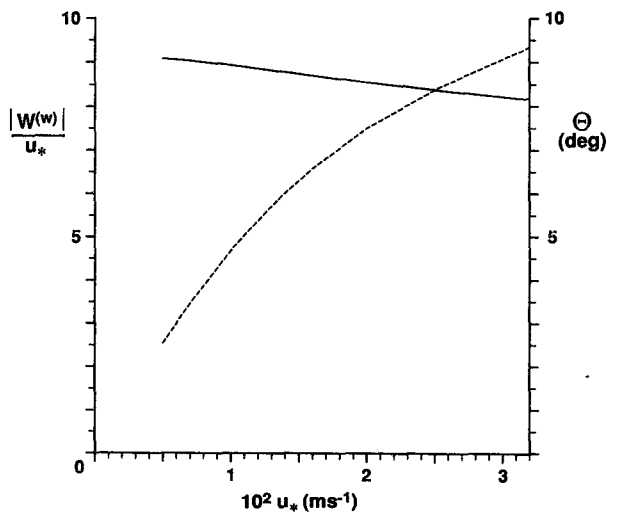

FIG. 6. Dimensionless wave-induced surface current speed $|W^{(w)}|/u_*$ (solid line) and deflection angle θ (dotted line) as functions of u_*, given at times when the fastest-growing wave component in question has reached a critical steepness; see the text for details.

9. Concluding remarks

In this study we have tried to formulate a theory for wind-driven ocean currents where we emphasize the dual role of the wind in transferring mean horizontal momentum to the ocean, that is, through a viscous drag at the sea surface in conjunction with the generation of surface waves. Our analysis is consistent in the way that air turbulence is responsible for the mean wind profile as well as for the normal stress fluctuations in phase with the wave slope that promote wave growth [for the wave-growth problem, see Knight (1977) and Jacobs (1987)]. For finite-amplitude, steep waves the secondary wave-induced mean motion in the air will alter the near-surface wind profile (Janssen 1989), but this effect is not taken into account here. Instead, our results are expressed as functions of the friction velocity, defined in terms of the mean tangential shear stress at the surface.

The present paper is focussed on the mean currents induced by growing wind waves. As demonstrated here, however, the viscous (eddy) dissipation in the ocean is not sufficiently effective to prevent the wave steepness of such waves from exceeding a critical limit. Accordingly, wave breaking must occur. In a fully developed sea state, the basic energy balance is between energy input from the wind and dissipation due to wave breaking. In addition, nonlinear wave–wave interactions may be important in this equilibrium range (Phillips 1985). A challenging future goal must be to model the drift current induced by waves in this regime.

REFERENCES

Banner, M. L., 1990: The influence of wave breaking on the surface pressure distribution in wind–wave interactions. *J. Fluid Mech.*, **211**, 463–495.

Bye, J. A. T., 1967: The wave drift current. *J. Mar. Res.*, **25**, 85–102.

——, 1988: The coupling of wave drift and wind velocity profiles. *J. Mar. Res.*, **46**, 457–472.

Chalikov, D. V., and V. K. Makin, 1990: Numerical approximation of wind–wave interaction parameter. *Ann. Geophys.*, Special issue, 197–198.

Charnock, H., 1955: Wind-stress on a water surface. *Quart. J. Roy. Meteor. Soc.*, **81**, 639–640.

Cheung, T. K., and R. L. Street, 1988: The turbulent layer in the water at an air–water interface. *J. Fluid Mech.*, **194**, 133–151.

Donelan, M. A., 1990: Air–sea interaction. *The Sea: Ideas and Observations on Progress in the Study of the Seas.* Vol. 9, B. LeMehaute and D. Hanes, Eds., Wiley-Interscience, 239–292.

Dore, B. D., 1978a: Some effects of the air–water interface on gravity waves. *Geophys. Astrophys. Fluid Dyn.*, **10**, 215–230.

——, 1978b: A double boundary-layer model of mass transport in progressive interfacial waves. *J. Eng. Math.*, **12**, 289–301.

Ekman, V. W., 1905: On the influence of the Earth's rotation on ocean currents. *Ark. Mat. Astron. Fys.*, **2**, 1–53.

Gaster, M., 1962: A note on the relation between temporally-increasing and spatially-increasing disturbances in hydrodynamic stability. *J. Fluid Mech.*, **14**, 222–224.

Hasselmann, K., 1970: Wave-driven inertial oscillations. *Geophys. Fluid Dyn.*, **1**, 463–502.

——, and Collaborators, 1973: Measurements of wind–wave growth and swell decay during the joint North Sea wave project (JONSWAP). *Dtsch. Hydrogr. Z.*, Erg. Heft **A12**, 96 pp.

Jackson, P. S., and J. C. R. Hunt, 1975: Turbulent flow over a low hill. *Quart. J. Roy. Meteor. Soc.*, **101**, 929–955.

Jacobs, S. J., 1987: An asymptotic theory for the turbulent flow over a progressive water wave. *J. Fluid Mech.*, **174**, 69–80.

Janssen, P. A. E. M., 1989: Wave-induced stress and the drag of air flow over sea waves. *J. Phys. Oceanogr.*, **19**, 745–754.

Jenkins, A. D., 1986: A theory for steady and variable wind- and wave-induced currents. *J. Phys. Oceanogr.*, **16**, 1370–1377.

——, 1987: Wind and wave induced currents in a rotating sea with depth-varying eddy viscosity. *J. Phys. Oceanogr.*, **17**, 938–951.

Kenyon, K. E., 1969: Stokes drift in random gravity waves. *J. Geophys. Res.*, **74**, 6991–6994.

Knight, D., 1977: Turbulent flow over a wavy boundary. *Bound.-Layer Meteor.*, **11**, 205–222.

Lamb, H., 1932: *Hydrodynamics*. 6th ed. Cambridge University Press.

Longuet-Higgins, M. S., 1953: Mass transport in water waves. *Phil. Trans. Roy. Soc. London*, **A245**, 535–581.

Maat, N., C. Kraan, and W. A. Oost, 1991: The roughness of wind waves. *Bound.-Layer Meteor.*, **54**, 89–103.

Madsen, O. S., 1977: A realistic model of the wind-induced Ekman boundary layer. *J. Phys. Oceanogr.*, **7**, 248–255.

McLeish, W. L., and G. E. Putland, 1975: Measurements of wind driven flow profiles in the top millimeter of water. *J. Phys. Oceanogr.*, **5**, 516–518.

Miles, J., 1957: On the generation of surface waves by shear flows. *J. Fluid Mech.*, **3**, 185–204.

——, 1962: On the generation of surface waves by shear flows. Part 4. *J. Fluid. Mech.*, **13**, 433–448.

Mitsuyasu, H., 1985: A note on the momentum transfer from wind to waves. *J. Geophys. Res.*, **90**, 3343–3345.

——, and T. Honda, 1982: Wind-induced growth of water waves. *J. Fluid Mech.*, **123**, 425–442.

Phillips, O. M., 1957: On the generation of waves by turbulent wind. *J. Fluid Mech.*, **2**, 417–445.

——, 1977: *The Dynamics of the Upper Ocean*. 2d ed. Cambridge University Press.

——, 1985: Spectral and statistical properties of the equilibrium range in wind-generated gravity waves. *J. Fluid Mech.*, **156**, 505–531.

Pierson, W. J., 1962: Perturbation analysis of the Navier-Stokes equations in Lagrangian form with selected linear solutions. *J. Geophys. Res.*, **67**, 3151–3160.

Plant, W. J., 1982: A relationship between wind stress and wave slope. *J. Geophys. Res.*, **87**, 1961–1967.

Shemdin, O. H., 1972: Wind-generated current and phase speed of wind waves. *J. Phys. Oceanogr.*, **2**, 411–419.

Snyder, R. L., F. W. Dobson, J. A. Elliot, and R. G. Long, 1981: Array measurements of atmospheric pressure fluctuations above surface gravity waves. *J. Fluid Mech.*, **102**, 1–59.

Stokes, G. G., 1847: On the theory of oscillatory waves. *Trans. Cambridge Philos. Soc.*, **8**, 441–455.

Thorpe, S. A., 1986: Measurements with an automatically recording inverted echo sounder; ARIES and the bubble clouds. *J. Phys. Oceanogr.*, **16**, 1462–1478.

Ursell, F., 1950: On the theoretical form of ocean swell on a rotating Earth. *Mon. Not. R. Astron. Soc., Geophys. Suppl.*, **6**, 1–8.

Weber, J. E., 1983: Steady wind- and wave-induced currents in the open ocean. *J. Phys. Oceanogr.*, **13**, 524–530.

——, 1990: Eulerian versus Lagrangian approach to wave-drift in a rotating ocean. *Kung. Vetenskaps och Vitterhets-Samhället, Göteborg, Acta: Geophys.*, **3**, 155–170.

——, and E. Førland, 1989: Effect of an insoluble surface film on the drift velocity of capillary-gravity waves. *J. Phys. Oceanogr.*, **19**, 952–961.

——, and ——, 1990: Effect of the air on the drift velocity of water waves. *J. Fluid Mech.*, **218**, 619–640.

Wu, J., 1975: Wind-induced drift currents. *J. Fluid Mech.*, **68**, 49–70.

——, 1982: Wind-stress coefficients over sea surface from breeze to hurricane. *J. Geophys. Res.*, **87**, 9704–9706.